

Unraveling the Room-Temperature Spin Dynamics of Photo-Excited Pentacene in its Lowest Triplet State at Zero Field

Hao Wu[†], Wern Ng[†], Shamil Mirkhanov[†], Arman Amirzhan[‡], Supamas Nitnara[†] and Mark Oxborrow^{ †}*

[†]Department of Materials, Imperial College London, Exhibition Road, London SW7 2AZ, U.K.

[‡]Harvard John A. Paulson School of Engineering and Applied Sciences, Harvard University, 29 Oxford Street, Cambridge, Massachusetts 02138, United States

Corresponding Author

*m.oxborrow@imperial.ac.uk

ABSTRACT

Photo-excited pentacene, upon arriving via intersystem crossing into its lowest triplet state, has been extensively studied due to the large and relatively long-lived spin polarization that it exhibits. However, the spin dynamics of these triplets has not hitherto been accurately determined, with glaring inconsistencies between published values. Using zero-field transient electron paramagnetic resonance (ZF-trEPR), we here report the determination of a complete set

of depopulation and spin-lattice relaxation rates for the lowest triplet state of pentacene doped at 0.1% into a *p*-terphenyl host crystal at room temperature in zero applied magnetic field. The rates of spin-lattice relaxation between the triplet's sublevels are found to be highly anisotropic (*i.e.* transition specific) and not negligible compared to the rates of depopulation from the same three sublevels back to pentacene's ground state. The spin dynamics as well as the ZF-trEPR technique reported here can aid the rational, quantitative engineering of applications such as room-temperature masers and triplet dynamic nuclear polarization (triplet-DNP).

INTRODUCTION

Pentacene can be substitutionally doped into certain organic molecular crystals during growth to form dilute solid solutions of individual, isolated pentacene molecules randomly dispersed within a host lattice. The lowest photo-excited triplet state of such pentacene, T_1 , exhibits high paramagnetic spin polarization at room temperature through triplet mechanism (TM)¹⁻³, *i.e.*, spin-selective intersystem crossing (ISC). Though naphthalene, benzoic acid and other molecules can be used, *p*-terphenyl is a popular choice for the host molecular crystal since it admits relatively high concentrations of pentacene (up to a few parts per thousand), is chemically inert (and thus relatively non-hazardous), and does not sublime at room temperature. Recent investigations have demonstrated the potential of pentacene-doped *p*-terphenyl (P:TP) in applications spanning triplet-DNP⁴⁻⁶, quantum computing⁷⁻⁸ and room-temperature masers⁹⁻¹⁰.

The origin of the pentacene's lowest triplet state in *p*-terphenyl is demonstrated in Figure 1a. With the optical excitation of 590 nm, the crystal's pentacene molecules are promoted from the ground state (S_0) to the first excited singlet state (S_1). Through spin-orbit coupling, molecules in S_1 will thereupon transfer over to the triplet state T_2 by resonant intersystem crossing (ISC) and

thereupon undergo rapid internal conversion (IC) to the lowest triplet state T_1 ¹¹, preserving their ISC-induced spin polarization. Anisotropic ISC rates, P_i ($i = x, y$ and z) lead to a highly non-Boltzmann initial population distribution across T_1 's three sublevels where $P_x: P_y: P_z = 0.76: 0.16: 0.08$ ¹. At room temperature and zero field, the three sublevels, T_x , T_y and T_z are non-degenerate whose splittings are determined by the zero-field splitting (ZFS) parameters of P:TP. The center frequencies of these splittings, namely T_x-T_z , T_y-T_z and T_x-T_y , are known to be 1.450 GHz, 1.344 GHz and 106.5 MHz, respectively¹².

The usefulness of P:TP (or any equivalent material exploiting TM) depends critically on the rate constants that determine the guest molecule's spin dynamics, namely: (i) the overall ISC yield¹³ together with the normalized population ratios¹ (three fractions adding up to unity) into T_1 's three sublevels, (ii) the rates of depopulation from these same three sublevels back to the ground state S_0 , and (iii) the rates of spin-lattice relaxation between these same three sublevels. Concerning (ii) and (iii), no accurate consensus has hitherto been arrived at as to their values. To complicate matters, almost all measurements of the depopulation and spin-lattice relaxation rates have, to date, been performed at high applied magnetic field^{1, 14-15}. Though the depopulation rates at zero field (ZF) can be inferred from their high-field equivalents (and *vice versa*) through projective mixing¹⁶⁻¹⁷; no straightforward relationship between the spin-lattice relaxation rates at zero and high field is available. Furthermore, the doping concentration of samples measured and reported is not always stated, rendering the identification of concentration effects/trends extremely difficult.

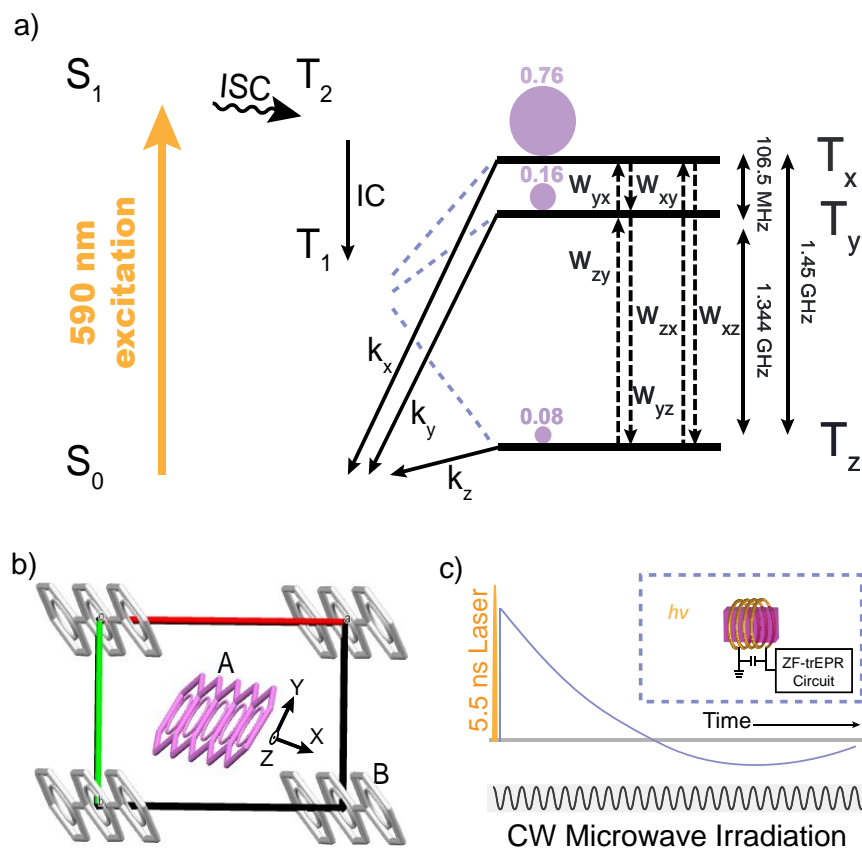


Figure 1. a) The processes associated with generating highly polarized pentacene triplets at ZF. Depopulation from the non-degenerate lowest triplet state, T_1 back to singlet ground state, S_0 and spin-lattice relaxations between the triplet sublevels are indicated by the one-way solid and dashed arrows, respectively. The relative populations of T_1 's three sublevels are represented by purple circles. b) A *p*-terphenyl unit cell with alternative doping sites A and B for pentacene at room temperature. The long in-plane axis, short in-plane axis and out-of-plane axis of pentacene molecule are denoted by X, Y and Z. c) The origin of a light-induced ZF-trEPR signal (purple trace). The inset is the schematic demonstration of ZF-trEPR technique in which a pentacene doped *p*-terphenyl crystal is loaded inside an LC circuit resonator.

Here, we provide accurate determinations of the depopulation and spin-lattice relaxation rates for the lowest photo-excited triplet state of 0.1% P:TP. This was achieved using trEPR at ZF. One

practical advantage of working at ZF is that no alignment with the crystal axes (Figure 1b) is required [*vis-à-vis* the precision goniometry (implemented through bespoke-angled wedges¹) needed for high-field measurements]. The depopulation rates of T₁'s non-degenerate sublevels, T_x, T_y and T_z were determined to be {k_x, k_y, k_z} = {2.8 ± 0.5, 0.6 ± 0.2, 0.2 ± 0.09} × 10⁴ s⁻¹. The rates of spin-lattice relaxation between these same three sublevels were determined to be {w_{xz}, w_{yz}, w_{xy}} = {1.1 ± 0.2, 2.2 ± 0.3, 0.4 ± 0.2} × 10⁴ s⁻¹. The meanings of k_i and w_{ij} (for i, j = x, y and z) are displayed in Figure 1a.

EXPERIMENTAL SECTION

Crystal Growth. Pentacene (TCI Europe NV) and *p*-terphenyl (Sigma-Aldrich, ≥99.5%) were purified by sublimation and zone-refining respectively prior to crystal growth. The purified pentacene and *p*-terphenyl were mixed in the mole ratio of 1:1000 and sealed in a cleaned borosilicate tube (inner diameter: 9 mm, Smith Scientific Ltd.) which was then evacuated for 3 hours and filled with Argon (BOC, 99.9999%). The mixed powder was melted in the central zone of a vertical tube furnace (Elite Thermal Systems Ltd.) at a temperature of 217 °C. Subsequently, a computer-controlled stepper motor (Velmex Inc.), lead screw, rail and translation stage (forming a vertical translator) were used to lower the sealed tube out of the furnace at a rate of 2 mm per hour. A pink crystal was formed after a 3-day growth run.

UV/Vis. The UV/Vis absorbance measurement of a polished P:TP crystal (with the thickness of 1 mm) was performed by a LAMBDA 750 UV/Vis/NIR Spectrometer.

ZF-trEPR Measurements. The P:TP crystal was placed within a suitably sized copper coil connected in parallel with an adjustable capacitor so forming an LC “tank” resonator (Figure 1c, inset), whose frequency was tuned to one of the material’s zero-field splittings shown in Figure

1a. By interrogating the P:TP-loaded tank resonator (loaded quality factor~30) with a microwave/VHF tone at one of these frequencies within a home-built Q -meter⁶ (= “bridge”) incorporating I-Q homodyne detection, the evolution of the difference in population (hence spin polarization) across each ZF splitting (= “transition”) could be detected as a function of time; see Figures 1c. The rf power level supplied to this bridge (controlling the amplitude of the oscillating magnetic field irradiating the crystal) was controlled by a cascade of in-line attenuators (inserted/removed by hand). The homemade broadband amplifier used in our ZF-trEPR circuit has the bandwidth of 10 MHz corresponding to the time resolution of 16 ns, which enables us to monitor fast dynamic processes in the sub-microsecond range. Supporting Information, particularly Figure S1, provides more details as to the anatomy of our ZF variant of a trEPR spectrometer¹⁸.

Optical Excitation. An optical parametric oscillator, OPO (Litron Aurora II Integra) pumped by its own internal Q-switched Nd:YAG laser was used to excite the P:TP crystal. The OPO was set to an output wavelength of 590 nm, a repetition rate of 10 Hz, and a pulse energy of 0.6 mJ. The pump laser’s Q-switching fixed the output pulse’s duration to 5.5 ns which was negligible in comparison to the timescale (microseconds) on which the subsequent spin dynamics evolves.

RESULTS AND DISCUSSION

According to the UV/Vis absorption spectrum of the 0.1% P:TP crystal shown in Figure 2, the characteristic absorption peak around 590 nm indicates the $S_0 - S_1$ transition of pentacene molecules. It agrees well with the theoretical calculations of the lowest optical absorption energy for P:TP crystals¹¹.

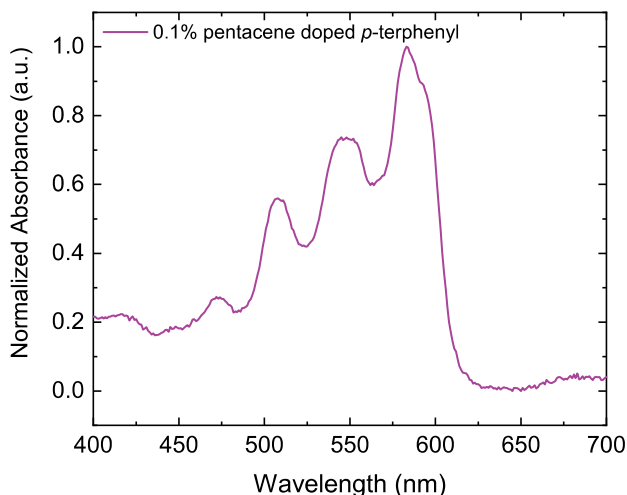


Figure 2. An UV/Vis spectrum of 0.1% pentacene doped *p*-terphenyl crystal

To achieve the least perturbed spin dynamics of pentacene’s lowest triplet state, we firstly investigated how the power level of the applied microwave tone affected the *Q*-meter’s (in-phase) output signal; see Figure 3. For all three ZF transitions, emissive signals appear initially, agreeing with the known population ratios into P:TP’s lowest triplet state¹. But since a less populated sublevel exhibits a longer lifetime, all three ZF transitions eventually become absorptive. Spin-echo studies (ESE) at high applied magnetic field (at room temperature) display analogous crossovers¹. And as with the study presented here, the time at which the signal crosses over (from emissive to absorptive) provides a robust, quantitative diagnostic.

In Figure 3, increasing the applied microwave power shortens the cross-over time, so hastening the demise of the emissive signal, for all three transitions. This arises due to an increased rate of stimulated transitions (both emission and absorption) with increasing applied microwave power. At high powers, both T_x - T_z and T_x - T_y signals exhibit transient nutations¹⁹, associated with strong coupling between the triplet spins and the electromagnetic field⁸. The observed transient

nutations revealing quantum oscillations have been thoroughly studied in the absence and in the presence of an external magnetic field based on theoretical models²⁰⁻²¹.

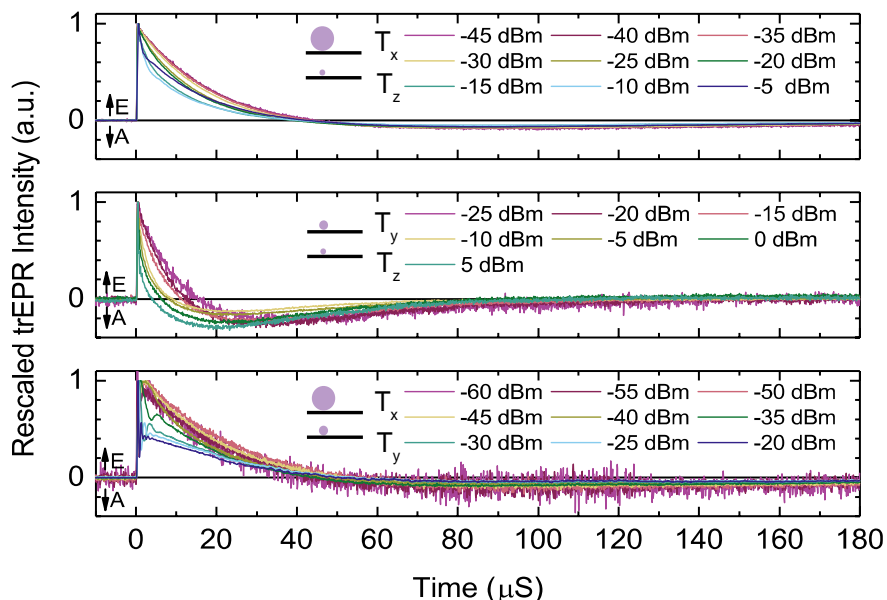


Figure 3. The microwave power effect on the trEPR signals at room temperature. The signals of the T_x - T_z , T_y - T_z and T_x - T_y transitions were obtained using resonators tuned at 1.45 GHz, 1.344 GHz and 106.5 MHz respectively. Signals have been shifted and rescaled such that their baselines lie at zero and their maximum positive vertical excursions reach 1 (in arbitrary vertical units). “E” denotes emissive and “A” denotes absorptive. The initial population distributions on the pentacene triplet sublevels according to the population rates stated in ref. 1 (reproduced in Table 1), are displayed in the insets.

In high-field experiments, that rate at which population in T_y decays back to S_0 was found to be comparable or smaller than the rate of decay from T_x ^{1, 14-15}. However, in Figure 3, even at the lowest applied microwave power (-25 dBm), the T_y - T_z trace still shows a much faster decay and shorter cross-over time compared to the traces for T_x - T_z and T_x - T_y . This observed rapid demise of the population difference across T_y - T_z implies rapid spin-lattice relaxation.

It can be seen that, after rescaling, the profile of each of the three measured ZF-trEPR signals changes little between the lowest few levels of applied power (*e.g.* for the T_x - T_z transition between -45 and -35 dBm). This indicates success in attaining the low-power limit for all three transitions, where stimulated emission, absorption and nutations can all be neglected. In this limit, the population dynamics should obey:

$$\dot{N}_x = -k_x N_x - w_{xz}(N_x - N_z) - w_{xy}(N_x - N_y)$$

$$\dot{N}_y = -k_y N_y - w_{yz}(N_y - N_z) - w_{yx}(N_y - N_x)$$

$$\dot{N}_z = -k_z N_z - w_{zx}(N_z - N_x) - w_{zy}(N_z - N_y)$$

Here, N_i is the population of the i -th sublevel. The kinetic parameters k_i and w_{ij} have the same meanings as those already introduced above (Figure 1a). Here, the rates of the upward and downward spin-lattice relaxations, w_{ij} and w_{ji} are assumed to be equal at room temperature (see Supporting Information for a justification of this assumption). The particular fitting procedure employed is explained in the Supporting Information. The six rate constants appearing in the above three equations were iteratively adjusted away from random sets of starting values –see Figure 4. All fits yielded R-squared values (indicating the goodness of fit) exceeding 0.99.

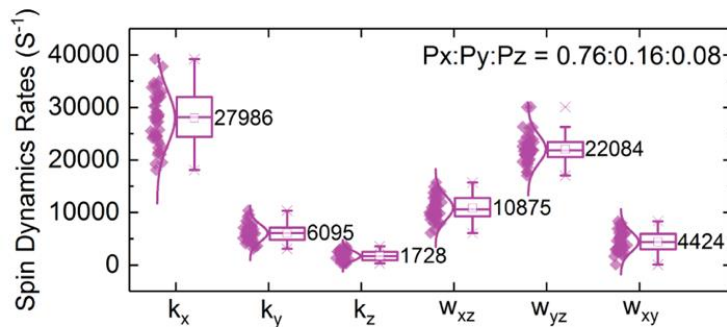


Figure 4. Best-fit values of the spin dynamics rates from different sets of starting values. The distribution of each fitted rate is represented by a box chart labelled with its mean value.

As shown in Figure 4, T_x offers the fastest decay back to the singlet ground state. In planar aromatic systems, the decay of the triplet sublevels to S_0 is dominated by non-radiative transitions²². Our result agrees well with theoretical considerations and calculations²³⁻²⁵ suggesting that the decays from T_x and T_y are non-radiative and driven by C-H and C-C vibrations respectively. Decay from T_z , on the other hand, results mainly from a slow radiative process. Although the fitted value for k_x has a relatively large standard deviation, it falls perfectly into the range reported for k_x as deduced from high-field measurements^{1, 15}. For completeness, we point out that the room-temperature value of k_x as well as those of other depopulation rates reported by Ong *et al.*¹⁴ are substantially larger than our values and those reported elsewhere (see Table 1).

Table 1. Room-temperature spin dynamics of pentacene triplets in *p*-terphenyl obtained at high field (H_0) and ZF. The units for k_i and $w_{i(j)}$ are 10^4 s^{-1} and H_0 is measured in T.

ISC yield, Φ_{ISC}							
62.5%							ref.13
Relative population rates, $P_x:P_y:P_z$							
0.76:0.16:0.08							ref.1
k_x	k_y	k_z	w_{xz} (w_3^a)	w_{yz} (w_2^a)	w_{xy} (w_1^a)	H_0	
$k_x + k_y$ $\sim 2.9 \pm 0.3^{b }$		0.1 $\pm 0.05^b$	0.7 $\pm 0.07^b$	2.6 $\pm 0.3^b$	1.9 $\pm 0.2^b$	~ 0.3	ref.1
9.7 ± 0.5	6.3 ± 1.9	0.9 ± 0.1	/	12.0 $\pm 0.9^c$	12.0 $\pm 0.9^c$	~ 0.3	ref.14
4.5 $\pm 0.4^d$	$k_y + k_z$ $\sim 2.3 \pm 0.4^{d }$		/	$< 0.3^d$	/	~ 0.3	ref.15
/	/	/	0.7 ± 0.1	/	/	0	ref.9
/	/	/	7.0 ± 1.0	/	/	0	ref.26

2.8 ±0.5	0.6 ±0.2	0.2 ±0.09	1.1 ±0.2	2.2 ±0.3	0.4 ±0.2
-------------	-------------	--------------	-------------	-------------	-------------

0 this work

^a w_1 is the spin lattice relaxation rate for $|0\rangle \leftrightarrow |+1\rangle$ transition, w_2 for $|0\rangle \leftrightarrow |-1\rangle$ and w_3 for $|-1\rangle \leftrightarrow |+1\rangle$ at high field.

^{b,c}rates were with $H_0//Z$.

^drates obtained with $H_0//X$.

^{||}this sum of two zero-field depopulation rates is deduced from the published high-field values through projection, namely: $k_{\pm 1} = \frac{1}{2}(k_x + k_y)$, $k_0 = k_z$ for $H_0//Z$ and $k_{\pm 1} = \frac{1}{2}(k_y + k_z)$, $k_0 = k_x$ for $H_0//X$.

Our most significant finding is that the rates of spin-lattice relaxation between the sublevels of the lowest triplet state in photo-excited P:TP at ZF are anisotropic, with magnitudes comparable to the sublevels' depopulation rates. Anisotropy across the spin-lattice relaxations was previously observed for P:TP at high field¹, though the high-field rates reported in ref. 1 (appearing in the top row of Table 1) cannot be direct connected to our own reported rates corresponding to zero applied field (bottom row of Table 1). In general, for the photo-excited triplet state, the anisotropic spin-lattice relaxation rates can be ascribed to phonon modulation of the electron dipolar interaction (zero-field splitting)²⁷⁻²⁸. In this case, the rates of spin-lattice relaxation scale monotonically with the transition frequency (ref. 27 and 28 consider a scaling in proportion to the splitting squared), then our results should obey the ordering $w_{xz} > w_{yz} > w_{xy}$. But they do not: from Figure 4, one observes that the spin-lattice relaxation across the T_y and T_z sublevels is the most rapid. We provide two possible mechanisms which may give rise to the exceptional fast spin-lattice relaxation of the T_y - T_z transition. First, at zero field, the first-order hyperfine interaction is zero, however, the perturbation of the second-order hyperfine interaction on the T_y -

T_z transition of P:TP can be observed from the multiple peaks resolved in the zero-field pulsed free induction decay (FID) EPR signal of the T_y - T_z transition, while one single peak was obtained for the T_x - T_z and T_x - T_y transitions¹². As the phonon modulation of the hyperfine interaction can contribute to the spin-lattice relaxation²⁹⁻³⁰, we assign this as one possible reason leading to the rapid spin-lattice relaxation of the T_y - T_z transition. Additionally, it was found that there is the rocking motion of the phenyl rings about the long-axis of *p*-terphenyl at room temperature³¹ which could drive the adjacent pentacene molecules to be distorted about their *x*-axis and thus promote the interactions of the spins on the T_y and T_z sublevels with the surrounding lattice.

A determination of w_{xz} deduced by simulating the response of an experimental maser⁹ agrees reasonably well with the value we report here: $(0.7 \pm 0.1) \times 10^4 \text{ s}^{-1}$ versus $(1.1 \pm 0.2) \times 10^4 \text{ s}^{-1}$. However, the value of w_{xz} reported in ref. 26 is anomalously high; we have no explanation other than to point out that the authors' model in this paper was two-level and thus could not have captured the full spin dynamics.

Based on the previously published determinations of the triplet-mechanism transition rates (i)-(iii) for P:TP (displayed in Table 1), it was surmised that bottlenecking (*i.e.* the build-up of population in the more slowly depopulating T_z sublevel –acting as the lower maser level) would preclude continuous (CW) masing across the T_x - T_z transition in P:TP^{9-10, 32}. Analysis shows that a certain figure of merit, κ , as was introduced in ref. 32, must exceed zero for continuous masing to be possible. Using our current best estimates within the black-lined rectangle of Table 1, we calculate κ to be -0.027 ± 0.084 . This indicates that 0.1% pentacene doped *p*-terphenyl most probably can't operate as a CW maser though lies tantalizingly close to the $\kappa = 0$ boundary.

Modifications such as deuteration of pentacene^{12, 14}, a different host crystal³¹, replacing pentacene by an aza-derivative of same (or of tetracene)³³, or even just a different doping concentration, could potentially nudge P:TP across into $\kappa > 0$ territory.

In summary, by means of ZF-trEPR, we have completely quantified the triplet-state spin dynamics of 0.1% pentacene doped *p*-terphenyl at room temperature for the first time. We observe that anisotropic spin-lattice relaxation, resulted from electron dipolar interaction and second-order hyperfine effect or rocking motion of phenyl rings in *p*-terphenyl, modifies the spin dynamics significantly. Our findings lay the foundations for rational designs of room-temperature masers and triplet-DNP systems based on the photo-excited triplet state of pentacene.

ASSOCIATED CONTENT

Supporting Information

The Supporting Information is available free of charge on the publisher's website.

AUTHOR INFORMATION

Corresponding Author

*m.oxborrow@imperial.ac.uk

Notes

The authors declare no competing financial interests.

ACKNOWLEDGMENT

This work was supported by the UK Engineering and Physical Sciences Research Council through grants EP/M020398/1 (Advanced Functional Materials) and EP/K037390/1 (Manufacturing Routes for Organic Room-Temperature MASER) H.W. acknowledges the China Scholarship Council (CSC) and Imperial College London for the CSC-Imperial PhD scholarship.

REFERENCES

1. Sloop, D. J.; Yu, H. L.; Lin, T. S.; Weissman, S. I. Electron-Spin Echoes of a Photoexcited Triplet: Pentacene in *p*-Terphenyl Crystals. *J. Chem. Phys.* **1981**, *75*, 3746-3757.
2. Henstra, A.; Lin, T. S.; Schmidt, J.; Wenckebach, W. T. High Dynamic Nuclear Polarization at Room Temperature. *Chem. Phys. Lett.* **1990**, *165*, 6-10.
3. Kagawa, A.; Negoro, M.; Ohba, R.; Ichijo, N.; Takamine, K.; Nakamura, Y.; Murata, T.; Morita, Y.; Kitagawa, M. Dynamic Nuclear Polarization using Photoexcited Triplet Electron Spins in Eutectic Mixtures. *J. Phys. Chem. A.* **2018**, *122*, 9670-9675.
4. Iinuma, M.; Takahashi, Y.; Shake, I.; Oda, M.; Masaike, A.; Yabuzaki, T.; Shimizu, H. M. Proton Polarization with *p*-Terphenyl Crystal by Integrated Solid Effect on Photoexcited Triplet State. *J. Magn. Reson.* **2005**, *175*, 235-241.
5. Tateishi, K.; Negoro, M.; Nishida, S.; Kagawa, A.; Morita, Y.; Kitagawa, M. Room Temperature Hyperpolarization of Nuclear Spins in Bulk. *Proc. Natl. Acad. Sci. U.S.A.* **2014**, *111*, 7527-7530.
6. Takeda, K. Studies on Dynamic Nuclear Polarization Using Photo-Excited Triplet Electron Spins. Ph.D. Thesis, Kyoto University, March 2005.
7. Lin, T. S.; Sloop, D. J.; Mou, C.-Y. Utilization of Polarized Electron Spin of Organic Molecules in Quantum Computing. *Int. J. Quantum Inf.* **2005**, *3*, 205-213.
8. Breeze, J. D.; Salvadori, E.; Sathian, J.; Alford, N. M.; Kay, C. W. Room-Temperature Cavity Quantum Electrodynamics with Strongly Coupled Dicke States. *npj Quantum Inf.* **2017**, *3*, 40.

9. Oxborrow, M.; Breeze, J. D.; Alford, N. M. Room-Temperature Solid-State Maser. *Nature* **2012**, *488*, 353-356.
10. Breeze, J.; Tan, K. -J.; Richards, B.; Sathian, J.; Oxborrow, M.; Alford, N. M. Enhanced Magnetic Purcell Effect in Room-Temperature Masers. *Nat. Commun.* **2015**, *6*, 1-6.
11. Bogatko, S.; Haynes, P. D.; Sathian, J.; Wade, J.; Kim, J. S.; Tan, K. J.; Breeze, J.; Salvadori, E.; Horsfield, A.; Oxborrow, M. Molecular Design of a Room-Temperature Maser. *J. Phys. Chem. C* **2016**, *120*, 8251-8260.
12. Yang, T. C.; Sloop, D. J.; Weissman, S. I.; Lin, T. -S. Zero-Field Magnetic Resonance of the Photo-Excited Triplet State of Pentacene at Room Temperature. *J. Chem. Phys.* **2000**, *113*, 11194-11201.
13. Takeda, K.; Takegoshi, K.; Terao, T. Zero-Field Electron Spin Resonance and Theoretical Studies of Light Penetration into Single Crystal and Polycrystalline Material Doped with Molecules Photoexcitable to the Triplet State via Intersystem Crossing. *J. Chem. Phys.* **2002**, *117*, 4940-4946.
14. Ong, J. L.; Sloop, D. J.; Lin, T. -S. Deuteration Effect on the Spin Dynamics of the Photo-Excited Triplet State of Pentacene in *p*-Terphenyl Crystals. *Chem. Phys. Lett.* **1995**, *241*, 540-546.
15. Kawahara, T.; Sakaguchi, S.; Tateishi, K.; Tang, T. L.; Uesaka, T. Kinetic Parameters of Photo-Excited Triplet State of Pentacene Determined by Dynamic Nuclear Polarization. *J. Phys. Soc. Jpn.* **2015**, *84*, 044005.
16. Schwöhrer, M.; Slxl, H. Optische Spin-Polarisation im Triplett-Zustand von Naphthalin. *Z. Naturforsch. A.* **1969**, *24*, 952-967.
17. Azumi, T.; O'donnell, C.; McGlynn, S. On the Multiplicity of the Phosphorescent State of Organic Molecules. *J. Chem. Phys.* **1966**, *45*, 2735-2742.
18. Weber, S. Transient EPR. *eMagRes*, **2017**, *6*, 255-270.

19. Kim, S. S.; Weissman, S. I. Transient Magnetization Following Photoexcitation. *Rev. Chem. Intermed.* **1979**, *3*, 107-120.
20. Yago, T.; Weidner, J. -U.; Link, G.; Lin, T. -S.; Kothe, G. Quantum Oscillations in Photo-Excited Triplet States in an External Magnetic Field. *Chem. Phys. Lett.* **2007**, *438*, 351-357.
21. Kothe, G.; Yago, T.; Weidner, J. -U.; Link, G.; Lukaschek, M.; Lin, T. -S.; Quantum Oscillations and Polarization of Nuclear Spins in Photoexcited Triplet States. *J. Phys. Chem. B* **2010**, *114*, 14755–14762;
22. Sixl, H.; Schwoerer, M. Dynamics of Optical Electron Spin-Polarization in Naphthalene. Magnetic Field Effects on Phosphorescence. *Chem. Phys. Lett.* **1970**, *6*, 21-25.
23. Henry, B.; Siebrand, W. Theory of Electron Spin Alignment through Nonradiative Processes in Naphthalene and Anthracene. *Chem. Phys. Lett.* **1970**, *7*, 533-536.
24. Siebrand, W. Mechanisms of Intersystem Crossing in Aromatic Hydrocarbons. *Chem. Phys. Lett.* **1970**, *6*, 192-194.
25. Henry, B. R.; Siebrand, W. Spin–Orbit Coupling in Aromatic Hydrocarbons. Analysis of Nonradiative Transitions between Singlet and Triplet States in Benzene and Naphthalene. *J. Chem. Phys.* **1971**, *54*, 1072-1085.
26. Salvadori, E.; Breeze, J. D.; Tan, K. -J.; Sathian, J.; Richards, B.; Fung, M. W.; Wolfowicz, G.; Oxborrow, M.; Alford, N. M.; Kay, C. W. Nanosecond Time-Resolved Characterization of a Pentacene-Based Room-Temperature MASER. *Sci. Rep.* **2017**, *7*, 41836.
27. Fischer, P. H. H.; Denison, A. B. Anisotropic Saturation of the Electron Spin Resonance in the Photo-Excited Triplet State of Pyrene-*d*₁₀. *Mol. Phys.* **1969**, *17*, 297-304.
28. Maruani, J. On Anisotropic Saturation of ESR Lines in Molecular Triplet States. *Chem. Phys. Lett.* **1970**, *7*, 29-30.
29. Panepucci, H.; Mollenauer, L. Spin-Lattice Relaxation of *F* Centers in Alkali Halides: Theory and Optical Measurements to 50 kG. *Phys. Rev.* **1969**, *178*, 589-598.

30. Cheng, C.; Lin, T. -S.; Sloop, D. J. Electron Spin-Echo Experiments of Diphenylnitroxide in Benzophenone Crystals. *J. Magn. Reson.* **1979**, *33*, 71-81.

31. Ong, J. L.; Sloop, D. J.; Lin, T. -S. Temperature Dependence Studies of the Paramagnetic Properties of the Photoexcited Triplet States of Pentacene in *p*-Terphenyl, Benzoic Acid, and Naphthalene Crystals. *J. Phy. Chem.* **1993**, *97*, 7833-7838.

32. Oxborrow, M. Maser assembly. US14/421,954, March 28, 2017.

33. Kouno, H.; Kawashima, Y.; Tateishi, K.; Uesaka, T.; Kimizuka, N.; Yanai, N. Non-Pentacene Polarizing Agents with Improved Air-Stability for Triplet Dynamic Nuclear Polarization at Room Temperature *J. Phys. Chem. Lett.* **2019**, *10*, 2208-2213.

Toc Graphics

